Electronic and optical properties of strained Ge/Si superlattices

U. Schmid, N. E. Christensen,* M. Alouani,† and M. Cardona
Max-Planck-Institut für Festkörperforschung, Heisenbergstrasse 1, D-7000 Stuttgart 80, Federal Republic of Germany
(Received 20 December 1990)

We present a comprehensive theoretical study of short-period $(\mathrm{Ge})_n/(\mathrm{Si})_m$ strained-layer superlattices (SLS's) on Si and Ge [001] substrates, and the "free-standing" case, based on *ab initio* calculations. In order to compensate for the error in the excitation energies inherent to the local-density approximation, we add *ad hoc* potentials on the atomic sites. With this correction the calculated transition energies compare favorably with quasiparticle calculations and experiment. Special emphasis is placed on the orthorhombic nature of the SLS's with both n and m even, as reflected in both the energy-band structure and the dielectric response $\epsilon_2(\omega)$, which is different for all three polarizations along the main axes. The effects of various substrates are examined for the occurring interband transitions, and in some cases reduced to a simple deformation-potential ansatz. A similar approach is taken for the splitting of the top of the valence band due to the internal uniaxial strain, which obeys a simple Vegard-type law; it is shown that confinement effects are negligible up to the values considered, i.e., $n+m=12$. The SLS's with a period of $n+m=10$ and sufficiently large strain in the Si layers have a direct gap; the transition from the top of the valence band to the lowest zone-folded conduction band at $\mathbf{k}=\mathbf{0}$, however, is only dipole allowed for special cases, such as the superlattices with n,m odd, i.e., for systems with no inversion symmetry. The $(\mathrm{Ge})_5/(\mathrm{Si})_5$ SLS is predicted to be a good candidate for optoelectronic devices. A reversal of the two lowest folded conduction states (dipole allowed and forbidden, respectively) is obtained when going from the $n=4$ to the $n=6$ case. Recent experiments on 10-monolayer SLS's are discussed in the light of our results.

I. INTRODUCTION

Ultrathin $(\mathrm{Ge})_n/(\mathrm{Si})_m$ strained-layer superlattices (SLS's) grown on Ge, Si, and $\mathrm{Ge}_x\mathrm{Si}_{1-x}$ buffers along the [001] direction have recently attracted considerable interest.[1] This is due to the multitude of design parameters that can be controlled during the growth with molecular-beam epitaxy, such as the period of SLS's $(n+m)$, the [Ge]/[Si] ratio (n/m), and the strain distribution within the two layers, which is—under pseudomorphic growth conditions—governed by the substrates (Ge, Si, or $\mathrm{Ge}_x\mathrm{Si}_{1-x}$ buffers).[1,2] Thus, the electronic and optical properties of these SLS's can be changed significantly and tailored to specific needs. Even more intriguing is the possibility to obtain a quasidirect band gap based on two indirect semiconductors, as has been conjectured by Gnutzmann and Clausecker.[3] Satpathy, Martin, and Van de Walle[4] have studied the electronic structure of Ge/Si SLS's by means of *ab initio* pseudopotential calculations. They suggested that an absolute conduction-band minimum is obtained for $(\mathrm{Ge})_n/(\mathrm{Si})_n$, $n=5,6$, when the SLS's are matched to Ge or $\mathrm{Ge}_{0.5}\mathrm{Si}_{0.5}$. Further support for a direct band-gap material based on Ge/Si SLS's with a period of 10-monolayer (ML) grown on Ge has been given by Pearsall *et al.*[5] In their experimental electroreflectance geometry, however, they could not excite the p_z polarization geometry, at which the direct transition is believed to occur. Zachai and co-workers[6,7] found strong photoluminescence in 10-ML period Ge/Si SLS's in the range 0.7 to 0.9 eV, when the Si layers are strained. The details of their interpretation, are, however, still under debate.[8] Both the electroreflectance and the photoluminescence measurements of the 10-ML SLS's present excellent experimental results, but further understanding has to be achieved on the basis of *ab initio* calculations.

The calculations reported here are performed within the local-density approximation (LDA) by means of the self-consistent (relativistic) linear-muffin-tin-orbitals (LMTO) method.[9,10] Like all methods based on the LDA, it suffers from the well-known "band-gap problem," i.e., the calculated excitation energies are notoriously underestimated. We correct for this error by including external potentials self-consistently in the calculations.[11] These *ad hoc* potentials have been determined for the bulk materials[12] and are transferred to the SLS's. This correction allows us to compare directly the excitation energies with recent experiments. We have shown earlier that the structure of the calculated dielectric function agrees well with spectroellipsometric measurements.[13]

We will present LMTO calculations of the band structure and dielectric function of Ge/Si SLS's with varying strain distribution, i.e., different substrates. The importance of the strain introduced in Ge/Si superlattices on their electronic band structures has been pointed out by various workers over the last years.[4,14–19] Recent LMTO calulations[20] of deformation potentials (DP's) in Si and

 ©1991 The American Physical Society

Ge have confirmed that the LMTO method gives reliable results for bulk materials under uniaxial and hydrostatic pressure, if compared to experiments. We thus have good reason to expect that this also holds for our SLS's calculations, both for the the zone-folded direct transitions at the Γ point of the SLS's [8] as well as interband transitions at higher energies, which determine the linear optical response of the SLS's.

Special emphasis is placed on the symmetry-related properties of these SLS's. In $(\mathrm{Ge})_n/(\mathrm{Si})_m$ SLS's with both n, m even, the Ge—Si bonds are all oriented parallel to one plane.[4] This means that those SLS's only have orthorhombic and not tetragonal symmetry.[21] Thus, the dielectric function $\varepsilon_2(\omega)$ is different for all three polarizations along the main axes, i.e., the SLS's are biaxial. The dominant anisotropy is of course given by the stacking effect along the growth direction, whereas the anisotropy perpendicular to the c axis is relevant for thin SLS's. It has been neglected in previous work.[22]

The paper is organized as follows. After a short introduction of the method we use for our band-structure calculations in Sec. II, we give a description of the symmetry properties and microscopic structure of the [001] SLS's considered in Sec. III. The consequences of the orthorhombic symmetry on the band structure and the dielectric response of the $(\mathrm{Ge})_2/(\mathrm{Si})_2$ SLS will be treated in Sec. IV. After a detailed discussion of the effects of the substrate on the optical properties of Ge/Si SLS's in Sec. V, the following section will concentrate on the conditions for obtaining quasidirect transitions in SLS's with a periodicity of 10 ML and dipole-allowed matrix elements, and compare recent experiments with the calculations. Finally, the paper ends with some concluding remarks in Sec. VII.

II. METHOD OF CALCULATION

The LMTO method which we use for our calculations is described in detail elsewhere.[9] The self-consistent potentials are created with a *scalar relativistic* Hamiltonian, including the "combined correction term."[9,23] Spin-orbit interaction is treated as a perturbation. Similar to the calculations of zinc-blende-type semiconductors, we include empty spheres, that is, atomic spheres with no nuclear charge, located at the tetrahedral interstitial sites in order to obtain a close-packed structure.[12]

In the atomic-sphere approximation (ASA), the sum of the sphere volumes (including empty spheres) has to equal the cell volume. This requirement, however, says nothing about the *ratio* of the atomic radii. In our calculation, we determined the sphere radii in the Si and Ge layers separately by calculating the volume of the two cuboids containing either all Si atoms or all Ge atoms. The plane separating the two cell parts (cuboids) was chosen to be in the middle of the Ge-Si interface. This procedure guarantees, that for sufficiently large SLS's grown on Si, the radii of the Si atoms and their empty spheres correspond to the Si bulk values, which is physically reasonable. We correct for the error in the band gaps introduced by the use of the LDA by the inclusion of extra *ad hoc* potentials placed at the atomic sites. These sharply peaked potentials are chosen so that the gaps at three symmetry points (Γ, X, L) of the bulk materials Si and Ge match the experimental data.[12] Although being of empirical nature, this procedure is in the spirit of the LDA. The empirical self-energy corrections are added as external potentials to the Hamiltonian thus participating in the self-consistent iteration scheme. The correction potentials were determined for the two bulk constitutents Si and Ge and then included in the self-consistent calculations for the SLS's, without altering them. This procedure has proven to yield very accurate results for the two bulk materials under strain,[20] and for other superlattices.[24,25] Although recent first-principles quasiparticle band-structure calculations by Hybertsen and Schlüter[15] with the self-energy interaction treated by the GW approximation may be physically more appealing, our method has the advantage of being computationally not quite as involved as theirs. Thus we can present here calculations of a wide range of Ge/Si SLS's as a function of multidimensional parameters, such as periodicity and strain distribution.

For the calculation of the complex dielectric function $\varepsilon_2(\omega)$, the self-consistent eigenvalues and wave functions (expressed in terms of the one-center expansion[9]) are used. Details of this method are published elsewhere.[26] The **k**-space integration is performed by means of the tetrahedron method[27] based on a sufficiently large number of **k** points in the irreducible Brillouin zone. For the SLS's investigated in this work, typically 500–700 points were used.

III. SYMMETRY AND STRUCTURE

The symmetry properties of $(\mathrm{Ge})_n/(\mathrm{Si})_m$ SLS's grown along the [001] direction have been studied in detail.[4,21] The extension to other growth directions is not straightforward.[28] Of particular interest to our study is the differentiation between tetragonal and orthorhombic symmetry. The latter occurs only if both indices n and m are even. In this case all Ge—Si bonds are oriented along the y direction as depicted in Fig. 1, whereas along the x direction only Si—Si and Ge—Ge bonds occur. The unit cells of these SLS with $\frac{1}{2}(n+m) =$ even are simple, biaxial orthorhombic [space group D_{2h}^5 $(Pmma)$], while those with $\frac{1}{2}(n+m) =$ odd are body centered [space group D_{2h}^{28} $(Imma)$].

If one of the indices n, m is odd, a fourfold rotation perpendicular to the layers exists, i.e., the symmetry becomes tetragonal. For $(n+m) =$ even, the same conditions for a simple [space group D_{2d}^5 $(P\bar{4}m2)$] and body-centered [space group D_{2d}^9 $(P\bar{4}m2)$] tetragonal unit cell hold as in the orthorhombic case.

Figure 2 shows the corresponding Brillouin zones of the SLS's inscribed in the parent zinc-blende Brillouin zone (BZ) in order to illustrate folding effects and to fa-

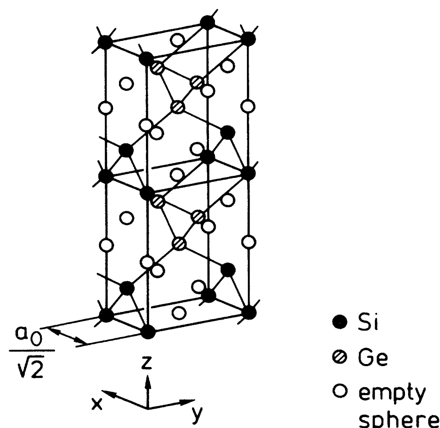

FIG. 1. Unit cell of the $(Ge)_2/(Si)_2$ SLS. The direction of the glide vector of the (001) glide planes is taken to be the x axis. Thus all Ge—Si bonds are oriented parallel to the yz plane in this case. Note that the $x-y$ axis is rotated by 45° with respect to those of the bulk with cells of Si and Ge.

miliarize the reader with the notation of the points of high symmetry. Note that the N point of the body-centered BZ [Fig. 2(b)] corresponds to the folded L point of the diamond BZ, and that the X point of the diamond BZ is referenced as M in the primitive orthorhombic BZ [Fig. 2(a)].

The investigation of the microscopic structure of Ge/Si SLS's has been very active during the last years.[29–32] Van de Walle and Martin[14] were the first to suggest on the basis of total-energy *ab initio* calculations, that the tetragonal distortions of the layers grown pseudomorphically on Si [001] substrate are in good agreement with the predictions of macroscopic elasticity theory. The strain is then fully confined in the Ge layers which are biaxially compressed by the lateral strain

$$\epsilon_{\parallel} = \frac{a_{\parallel}}{a_i} - 1 , \tag{1}$$

and expanded perpendicular to the interface by

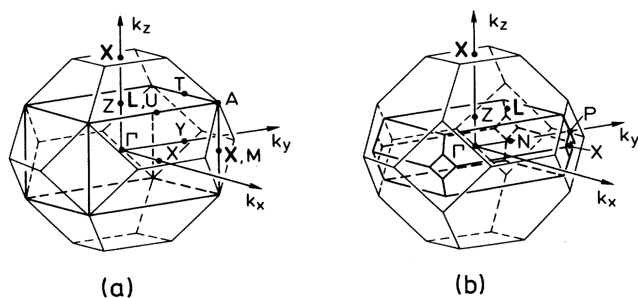

FIG. 2. Brillouin zone of superlattices (thick line) embedded in the parent zinc-blende Brillouin zone, for which the corresponding **k** points are shown in bold. (a) Primitive BZ for $\frac{1}{2}(n+m)=2$ (even); (b) body-centered BZ for $\frac{1}{2}(n+m)=3$ (odd).

$$\epsilon_{\perp} = \frac{a_{\perp}}{a_i} - 1, \tag{2}$$

where a_i, $a_{\parallel}$, and $a_{\perp}$ are the equilibrium (bulk) lattice constants of the strained material (i = Ge), of the substrate (Si), and the lattice spacing perpendicular to the interface, respectively. Commensurate growth ensures that the lattice constant parallel to the interface $a_{\parallel}$ remains the same throughout the structure. The extension along the growth direction is governed by the elastic response of the strained material and can be calculated via[33]

$$\Delta = \frac{a_{\perp}}{a_{\parallel}} - 1 \approx \epsilon_{\perp} - \epsilon_{\parallel} = -\epsilon_{\parallel}\left(1 + \frac{2C_{12}}{C_{11}}\right), \tag{3}$$

where C_{11},C_{12} are the elastic stiffness constants of the strained material.

The strain tensor $\overleftrightarrow{\epsilon}$ can be decomposed into a hydrostatic and a uniaxial component:

$$\overleftrightarrow{\epsilon} = \begin{pmatrix} \epsilon_{\parallel} & 0 & 0 \\ 0 & \epsilon_{\parallel} & 0 \\ 0 & 0 & \epsilon_{\perp} \end{pmatrix} = \epsilon_h \begin{pmatrix} 1 & 0 & 0 \\ 0 & 1 & 0 \\ 0 & 0 & 1 \end{pmatrix} + \epsilon_u \begin{pmatrix} -1 & 0 & 0 \\ 0 & -1 & 0 \\ 0 & 0 & 2 \end{pmatrix} . \tag{4}$$

The hydrostatic part ϵ_h has Γ_1 symmetry and shifts various direct and indirect band gaps,[20] without splitting essential degeneracies, whereas the uniaxial, traceless component ϵ_u (Γ_{12} symmetry) splits the valence-band top (VBT) at $\mathbf{k}=\mathbf{0}$ and introduces an anisotropy among the $k_{x,y}$ and k_z directions, thus splitting previously degenerate bands. In the case of strained Ge layers on Si substrate ($a_i = a_{\mathrm{Ge}}$, $a_{\parallel} = a_{\mathrm{Si}}$), we obtain for the tetragonal distortion $\Delta = 7.3\%$, and $\epsilon_h = -1.65\%$, $\epsilon_u = 2.35\%$ ($\Delta \approx 3\epsilon_u$).

This macroscopic strain consideration, however, covers only the spacing of the strained layers and leaves the important question for the interface spacing (separation between the Ge and Si layers) open. Also, for short-period SLS's, the individual interlayer spacings do not have to be constant for all layers, but may vary slightly. While Van de Walle and Martin[14] took for the interface spacing d(Ge—Si) the average of the layer spacings of the two cubic bulk materials, Hybertsen and Schlüter[15] fixed the Ge—Si bond length to be the average of the cubic Si—Si and the strained (expanded) Ge—Ge bond length.

Recent valence-force-field (VFF) calculations,[16,31] based on *ab initio* and experimental force constants, and self-consistent total-energy pseudopotential calculations[30] give a more detailed picture of the individual interlayer spacings. They are presented in Table I together with the results we obtained by relaxing the SLS structures with a valence-force-field scheme,[34,35] using the experimental force constants[35] α, and β for Si-Si, Ge-Ge, and the geometric average for the Ge—Si bonds.

TABLE I. Tetragonal distortion $\Delta = (a_{\perp}/a_{\parallel} - 1)$ in percent of the various interlayer spacings for $(Ge)_n/(Si)_n$ SLS pseudomorphically grown on [001] substrate (a_{Si}, free standing $\bar{a}$, and a_{Ge}). In the present work, the geometry was obtained by minimization of the strain energy in a valence-force-field scheme, using the experimental force constants α(Si-Si) = 48.50 N/m, α (Ge-Ge) = 38.67 N/m, α(Ge-Si) = 43.31 N/m, β (Si-Si) = 13.81 N/m, β(Ge-Ge) = 11.35 N/m, and β (Ge-Si) = 12.52 N/m, and lattice parameters (for $a_{\parallel}$) a_{Si} = 5.431 Å, a_{Ge} = 5.657 Å, and $\bar{a}$ = 5.531 Å (free-standing case).

		Δ (Si-Si)			Δ (Ge-Si)			Δ (Ge-Ge)		
$a_{\parallel}$		a_{Si}	$\bar{a}$	a_{Ge}	a_{Si}	$\bar{a}$	a_{Ge}	a_{Si}	$\bar{a}$	a_{Ge}
$n = 2$	Present work	−0.27	−3.50	−7.39	3.65	0.39	−3.53	7.54	4.26	0.29
	From Ref. 31[a]	−0.26		−7.71	3.74		−3.60	7.49		0.30
	From Ref. 16[b]	−0.27	−3.43	−6.51	2.96	−0.18	−3.26	6.31	3.23	0.23
$n = 4$	Present work	0.03 −0.14[c]	−3.18 −3.35[c]	−7.05 −7.24[c]	3.64	0.39	−3.54	7.26 7.42[a]	3.96 4.13[c]	−0.03 0.15[c]
	From Ref. 31[a]	−0.11 0.05[c]		−7.56 −7.39[c]	3.66		−3.60	8.05 7.38		0.22 −0.02[c]
	From Ref. 16[b]	−0.01 −0.15[c]	−3.14 −3.30[c]	−6.21 −6.37[c]	2.98	−0.17	−3.24	6.06 6.20[c]	2.92 3.12[c]	−0.06 0.11[c]
	From Ref. 30[d]	0.0 − 0.6[a]			2.7			5.5 5.2[c]		
	From Refs. 14 and 15[e]	0.0	−2.90	−6.9	3.6		−3.4	7.2	4.2	0.0

[a]VFF with experimental parameters.
[b]VFF with *ab initio* parameters.
[c]Occurs twice due to symmetry.
[d]LDA total-energy calculation.
[e]Macroscopic elasticity theory, confirmed by LDA.

Values are given for commensurate growth of $(Ge)_n/(Si)_n$ SLS's on three different substrates with the lattice constants, a_{Si}, a_{Ge}, and $\bar{a}$. The latter refers to the "free-standing" case, i.e., the state the SLS would adopt for a minimum of elastic energy.[14] In general, the results compare well, confirming, that the Ge—Si bond length at the interface is approximately the average of the *strained* Si—Si and Ge—Ge bond lengths.

One should point out that the Keating model, as used in the present context here and in other works, is simply a harmonic model in which explicit linear terms in $(r - r_0)^2$ are not included. While anharmonic terms are not expected to give large deviations from the calculated parameters the neglect of linear terms could. Although the Keating model is often used to determine equilibrium lattice parameters, one should realize that one does not have any control over the possible effect of explicit linear terms. Existing *ab initio* total-energy calculations,[30,32] however, lead to poor agreement of the lattice constants $a_{\perp}$ with those calculated from the elastic constants. This is related to an underestimated lattice mismatch between bulk Si and Ge in the *ab initio* calculations.[32] Thus, the lattice constants $a_{\perp}$ derived from simple elasticity theory, which are exactly reproduced by the Keating model (see Table I), compare better to channeling experiments.[36] For this reason we use Keating model parameters in our calculations while we emphasize the need for experimental determination of the interlayer spacings.

We obtain for the $(Ge)_4/(Si)_4$ SLS a small "overshoot" of the Ge-Ge distances in the two Ge layers next to the interface with respect to the central Ge plane, in contrast to the Si side, where the situation is reverse.[37] The absolute magnitude of these differences, however, is extremely small (<0.003 Å) and shifts the energies by $\leq$ 20 meV, if compared to calculations for geometries without oscillations.

Table II shows the results of our valence-force-field calculations for the interlayer spacing of 10-ML SLS's ($n + m = 10$, $4 \leq n \leq 6$). Note how the symmetry of the SLS's is reflected in the displacement values. The difference of the displacements obtained for smaller SLS's as described in Table I are marginal.

IV. ANISOTROPY OF ORTHORHOMBIC SUPERLATTICES

Equipped with the formalism described in Sec. II, we performed fully relativistic band-structure calculations of various SLS's for different strain distributions. Results for the $(Ge)_2/(Si)_2$ SLS on Si [001] substrate are depicted in Fig. 3. The calculated lowest transition of the $[(Ge)_2/(Si)_2]$/Si SLS is clearly indirect (E_g = 0.90 eV at $0.95M$), while the lowest direct transitions at Γ occur at 1.36 and 1.55 eV; their matrix elements are two orders of magnitude below that of the *unfolded* E_0 transition at 2.49 eV. This system is of particular interest as it is the shortest-period Ge/Si SLS with orthorhombic symmetry. We see in Fig. 1 that all Ge—Si bonds are oriented parallel to the yz plane, whereas parallel to the xz plane Si—Si and Ge—Ge bonds alternate. For a $Ge_{2k}Si_{2l}$ SLS (k, l = 1,2,3,. . .,) the proportion of Ge—Si bonds parallel

TABLE II. Tetragonal distortions (compare Table I) for $(Ge)_n/(Si)_m$ SLS's ($n+m=10$) as calculated within the valence-force-field scheme. $\bar{a}$ refers to the free-standing case, with $\bar{a}=5.509$ Å ($n=4$), $\bar{a}=5.531$ Å ($n=5$), and $\bar{a}=5.554$ Å ($n=6$).

	Δ(Si-Si)			Δ(Ge-Si)			Δ(Ge-Ge)		
$a_{\parallel}$	a_{Si}	$\bar{a}$	a_{Ge}	a_{Si}	$\bar{a}$	a_{Ge}	a_{Si}	$\bar{a}$	a_{Ge}
$(Ge)_4/(Si)_6$	0	−2.52	−7.08				7.26	4.68	−0.03
	0.01[a]	−2.49[a]	−7.06[a]	3.64	1.10	− 3.54	7.42[a]	4.84[a]	0.15[a]
	−0.14[a]	−2.65[a]	−7.23[a]						
$(Ge)_5/(Si)_5$	0.01[a]	−3.19[a]	−7.06[a]	3.64	0.39	−3.54	7.28[a]	3.98[a]	−0.01[a]
	−0.14[a]	−3.35[a]	−7.23[a]				7.42[a]	4.13[a]	0.15[a]
$(Ge)_6/(Si)_4$	0.03	−3.90	−7.05				7.29	3.25	0
	−0.14[a]	−4.07[a]	−7.24[a]	3.64	−0.34	−3.54	7.28[a]	3.24[a]	−0.01[a]
							7.42[a]	3.39[a]	0.15[a]

[a]Occurs twice due to symmetry.

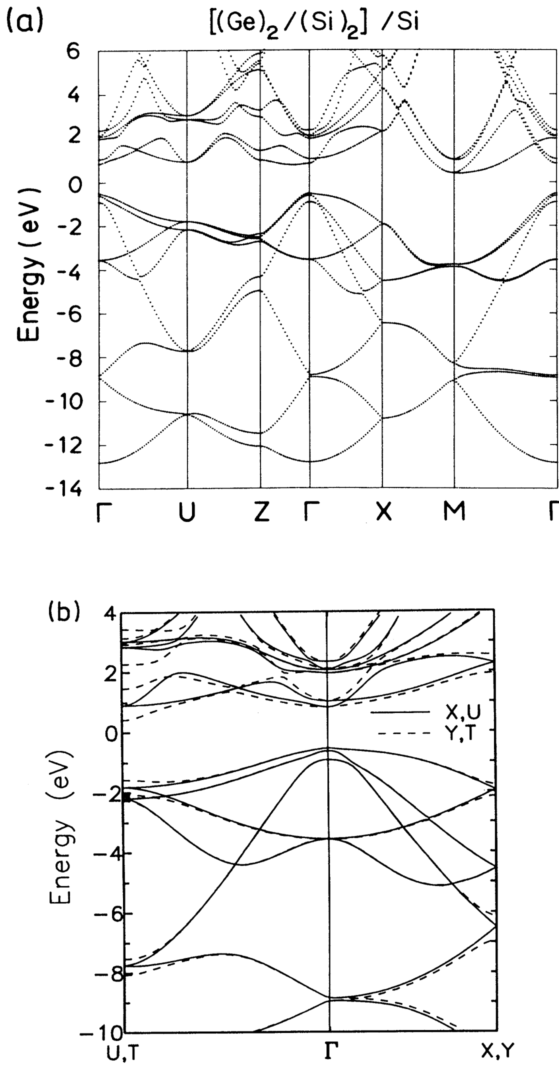

FIG. 3. (a) Fully relativistic band structure of the $[(Ge)_2/(Si)_2]/Si$ [001] superlattice along lines of high symmetry. (b) Details of the band structure along certain directions that demonstrate the orthorhombicity of the $(Ge)_2/(Si)_2$ SLS.

to the yz plane amounts to $2/(k+l)$ and thus decreases with increasing periodicity.

Because of its nonsymmorphic space group (D_{2h}^5), a group theoretical analysis shows that all bands are doubly degenerate (not counting the spin degeneracy) at the X and U points, but not at the Y and T points.[38] In the tetragonal primitive BZ, the X and Y points are equivalent, just as the U and T points (the latter are called R). At the Y and T points, the valence bands split up by typically 0.5 eV [see Fig. 3(b)]. Note that the highest valence band is folded back at the boundary of the BZ when compared to that of the zinc-blende structure. Except for the **k**-space region very close to the edge of the BZ, the valence states remain basically unaffected, reflecting the similarity of the valence states in Si and Ge bulk materials. This is not the case for the conduction bands. The difference is most pronounced for the s like lowest conduction states due to the relativistic downshift with increasing mass. A difference of $0.1-0.2$ eV can be observed in the two lowest energy bands ("original" and folded one) with s character along the two inequivalent directions in **k** space for the $[(Ge)_2/(Si)_2]/Si$ SLS. The effects of the anisotropy in the bands can readily be observed in the imaginary part of dielectric function, $\varepsilon_2(\omega)$, which is presented in Fig. 4 for all three polarizations along the main axes. It should be mentioned that similarly to bulk materials the calculated magnitude of the E_1 transition is strongly underestimated, when compared to experiments.[13] This is due to excitonic and other many-body effects, which are neglected in the calculations.[26] The major anisotropy in $\varepsilon(\omega)$ originates from the different strain distribution along the z and x,y axes, which has complicated effects on the critical points and their matrix elements. The main difference between the $p_{x,y}$ and p_z occurs in the energy range from $\approx 3-4.5$ eV at the critical points E_1 and E_2, and not so much above and below these energies. This is in good agreement with earlier semi-*ab initio* linear combination of Gaussian orbitals (LCGO) calculations.[22] The authors of Ref. 22 have pointed out that the gross features of the $(x,y)-z$ anisotropy can be explained in terms of strained bulk materials. They estimated the ratio $\varepsilon_2^{zz}/\varepsilon_2^{xx,yy}$ with a simple

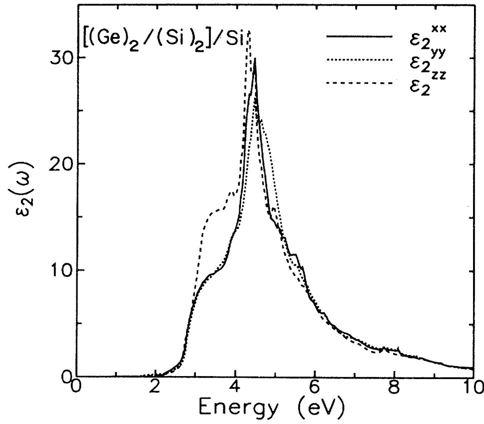

FIG. 4. Imaginary part of the dielectric response $\varepsilon_2(\omega)$ for the $[(Ge)_2/(Si)_2]/Si$ SLS for the three principal polarizations.

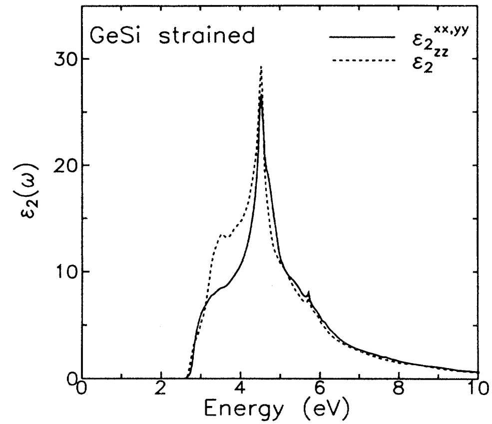

FIG. 5. $\varepsilon_2(\omega)$ of the zinc-blende-like compound "GeSi" with the total (averaged) strain calculated for a SLS on a Si substrate

tight-binding argument to be ≈ 1.15. We see in Fig. 4 that this ratio is a complicated function of the energy and varies from 1.0 to 1.4. The ratio of the integrated ε up to an energy of 10 eV amounts to 1.08.

In contrast to the strained bulk calculation[22] we used a different approach to relate the anisotropy in the 3–4-eV region to a tetragonal distortion: we transferred the averaged strain of the Ge and Si layers to the zinc-blende like "GeSi" compound, i.e., a $(Ge)_1/(Si)_1$ superlattice.[12] The dielectric response of this material which contains macroscopically the same strain as the $(Ge)_n/(Si)_n$ SLS is shown in Fig. 5. This now is a truly tetragonal system and thus has only two polarizations for $\varepsilon_2(\omega)$. The increase in the oscillator strengths for the zz polarization in the energy range from $3-4$ eV is quantitatively in good agreement with that of the $[(Ge)_2/(Si)_2]/Si$ SLS. The structure in the dielectric response of this complex system is of course much richer than that of the simple "GeSi." A clear difference can be observed below 2.7 eV, where GeSi has no structure, but $[(Ge)_2/(Si)_2]/Si$ shows strong absorption from a multitude of bands.

Although the $(x,y)-z$ anisotropy arising from the tetragonal distortion is rather large, the orthorhombic $x-y$ anisotropy is small, and the integrated difference of the $(x-y)$ amplitudes is zero. The $(x-y)$ difference occurs mainly between 4.2 and 5.2 eV and can readily be explained on the basis of the band structure shown in Fig. 3(b). Although most of the contributions to the large E_2 peak at ≈ 4.4 eV originate in transitions from the VBT ($v1$, counting from the VBT downwards) to the lowest conduction band ($c1$, counting upwards) at $\approx \frac{4}{5}M$ in $\mathbf{k}$ space, there are also contributions from the $v2$, $v3$ bands to $c2$ at $\approx \frac{1}{2}X, Y$ and from $v3$ to $c2$ at $\frac{2}{3}U, T$. The difference in band energies and joint density of states is reflected in a shift of the position and strengths of ε for the two polarizations. This also holds for the energy region around 5 eV, which contains contributions from $v2$ to $c4$ transitions at $k \approx \frac{3}{4}U, T$.

Similar effects can be observed in all orthorhombic $(Ge)_{2k}/(Si)_{2l}$ SLS's. With an increasing number of bands, however, the analysis and the assignment to specific interband transitions becomes more difficult. We thus concentrated on the "simple" case $(Ge)_2/(Si)_2$. The splitting at the BZ boundary for larger orthorhombic SLS's will be discussed in Sec. V. We should, however, keep in mind that even for these larger systems the difference in the conduction states $c1$ and $c2$ can reach values up to 0.3 eV, and thus are, together with the splitting of the valence states at the BZ boundary, not negligible in all cases.

V. EFFECTS OF THE SUBSTRATE

The $[(Ge)_4/(Si)_4]/Si$ [001] SLS is the SLS that has been investigated the most since the electroreflectance measurement by Pearsall and co-workers.[1] Its electronic structure has been calculated by various methods[15–19] over the last years. We present its energy-band structure as calculated with the LMTO method together with its counterpart on a Ge substrate in Fig. 6. Notice the splitting of the bands at the Y and T points, similar to that found for the 2×2 structure.

Note that in order to keep the X point as that where all bands are doubly degenerate we must define the x direction of real space such that the glide vectors of the (001) glide planes are along x. This has the effect of rotating the Ge—Si bonds of Fig. 1 $[(Ge)_2/(Si)_2]$ by 90° around z.

The uniaxial strain component ϵ_u splits the VBT Γ_8^+ doublet of the bulk correspondingly in the case where the Si layers are strained [Ge substrate, Fig. 6(b)], the $|\frac{3}{2},\frac{1}{2}\rangle$ ($v1$) state is now above that of the $|\frac{3}{2},\frac{3}{2}\rangle$ ($v2$). This implies that transitions originating from the uppermost valence state at $\mathbf{k}=\mathbf{0}$ will be mainly z polarized, and not x or y as in the Si substrate case. The energy difference between the v_2 and v_1 amount to 0.10 eV for the $[(Ge)_4/(Si)_4]/Si$, and to -0.18 eV for the

$[(Ge)_4/(Si)_4]/Ge$. A detailed analysis of these splittings will be given in Sec. V B.

Table III shows the dipole-allowed transition energies of the $(Ge)_4/(Si)_4$ SLS's for three different substrates (Si, Ge, and free standing). In the case of the Si substrate, the LMTO results are compared to electroreflectance data by Pearsall *et al.*[1] and quasiparticle calculations (QP) by Hybertsen and Schlüter.[15] As can be verified in Table III, the zone-folded (ZF) and E_0 direct transition energies at $\mathbf{k} = \mathbf{0}$, as well as the transitions, that can be assigned to the strain-split bulklike E_1 gaps agree within 0.1 eV in this comparison. This cleary demonstrates the validity of our assumption, that the the adjusting external potentials can be transferred from the bulk materials to the corresponding atomic postions in the SLS's. Both the LMTO method with adjusting potentials and the QP calculations give equally good results in the calculation of excitation energies in SLS's. We should, however, keep in mind, that all of these calculations assume an idealized system, namely an infinitely extended SLS with a sharp interface. The sample prepared by Pearsall *et al.* consists of a quantum-well structure of Si and 4 – 5 periods of $(Ge)_4/(Si)_4$ SLS. The additional confinement effects of such a system could explain that the calculated values are almost systematically 0.05 eV above the measured ones, although such small absolute values are beyond the limit of accuracy of the calculations [the transverse mass at the X point of bulk Si ($0.2m_0$) is much smaller than the longitudinal mass]. The transitions from the VBT to the lowest ZF band are dipole forbidden in all three substrate cases.[4] The first allowed direct transitions have calculated matrix elements that are 3–4 orders of magnitudes below that of the E_0 transition.

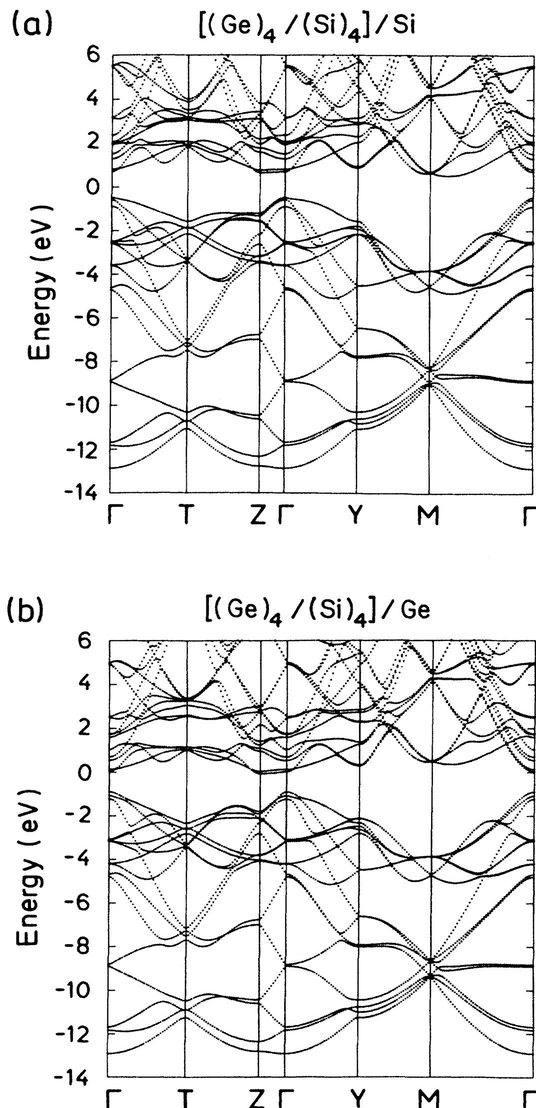

FIG. 6. Energy-band structure of the $(Ge)_4/(Si)_4$ superlattice for pseudomorphic growth on (a) Si [001] and (b) Ge [001] substrate along lines of high symmetry.

In addition to the energy range previously reported in the literature we list transitons up to 5 eV in Table III, and extend the discussion to other substrates than Si. We have shown earlier[13] that transitions in the range above ≈ 3.3 eV and below the E_2 edge can be ascribed to superlattice transitions, such as these which originate from the k_z direction. These transitions, however, are very weak.

The E_1-like transitions around 3 eV are much stronger. The calculated energies are around the value reported for the E_1 gap of the zinc-blende like "GeSi" material,[12] namely, ≈ 2.8 eV. Due to the difference of ≈ 1.2 eV between these transitions in the two bulk materials Ge and Si and the variety of strain-split and folded bands, they split into various components in the case of the SLS, and thus become rather broad. This is illustrated in Fig. 7(a), where the average of the ε_2^{xx} and ε_2^{yy} dielectric responses, is plotted (the difference between ε_2^{xx} and ε_2^{yy} is even smaller than in the $n = 2$ case, so that we can concentrate on uniaxial anisotropy due to the different substrate and the tetragonal distortion). Thus, the $\varepsilon_2^{zz}(\omega)$ functions for SLS's grown on Si as well as Ge substrates are presented in Fig. 7(b). In contrast to the case of the Si substrate, where the amplitude of the ε_2^{zz} in the energy range from $\approx 2.5 - 4$ eV is significantly larger than that of $\varepsilon_2^{xx,yy}$, as discussed in the case of the $(Ge)_2/(Si)_2$ SLS, the situation reverses for the Ge substrate. The magnitude of the enhancement of $\varepsilon_2^{xx,yy}$ over ε_2^{zz} in that energy range also reaches up to 45%. Note that the germanium E_1-like edge seen in Fig. 7 at ≈ 2.3 eV shows a sign of the $(x,y) - z$ anisotropy in agreement with that which is predicted by the uniaxial stress in the Ge layers, i.e., a decrease (increase) of its magnitude for lateral compression in x,y (z) polarization. According to the data in Ref. 39 we predict that this edge should be lower for x,y than for z polarization.

The E_2 transitions exhibit pronounced bulklike peaks with weak satellites. This is because the bulk Si and Ge E_2 transitions nearly fall together. The peaks of all critical points are shifted upward in energy for Si substrate.

TABLE III. Transition energies of $(Ge)_4/(Si)_4$ superlattices. The LMTO results are compared (if possible) to quasiparticle calculations (QP, see Ref. 15) and electroreflectance data. ZF refers to transitions that arise as a result of zone folding at $\mathbf{k} = \mathbf{0}$. The transitions between the E_1 and E_2 peaks are referred to as superlattice ("SL") transitions. Note that the $[(Ge)_4/(Si)_4]/Si$ at $\mathbf{k} = 0$ transitions originate from v_2 and thus are p_x, p_y polarized, in contrast to the transitions of the $[(Ge)_4/(Si)_4]/Ge$ and free-standing case, which are p_z polarized and stem for v_1.

	$[(Ge)_4/(Si)_4]/Si(001)$			$(Ge)_4/(Si)_4$ free standing	$[(Ge)_4/(Si)_4]/Ge(001)$
	LMTO[a]	QP[b]	expt.[c]	LMTO[a]	LMTO[a]
E_g	0.99	0.85	0.76		0.84
ZF	1.29	1.24	1.25	1.30	1.03
ZF	1.78	1.76	1.70	1.75	1.43
E_0	2.43	2.40	2.20,2.38	2.35	1.93
E_1	2.27,2.43	2.50		2.31,2.48	2.37
	2.65[d]	2.55	2.60	2.68[d]	2.51[d],2.65
	2.84,2.91	2.88	2.82	2.68	2.88
		3.18,3.20	3.04	3.01	3.10
	3.23	3.24,3.28	3.22	3.26	3.19
SL	3.47			3.40	3.42
	3.68			3.60	3.62,3.75
	3.84			3.79,4.08	3.98
	4.19			4.22	4.19
E_2	4.39[d]			4.37[d]	4.29[d]
	4.62			4.58	4.49
	4.76			4.78	4.65
	4.90			4.90	4.89

[a]Present work.
[b]Quasiparticle calculations, Ref. 15.
[c]Electroreflectance, Ref. 1.
[d]Dominant, bulklike transition.

This can be explained in terms of a hydrostatic compression of the Ge layers, which in combination with negative values for all hydrostatic DP's $a(E_i) = dE/d\ln V$ results in an shift towards *higher* energies.

The peaks in ε_2^{zz} are sharper than those of ε_2^{xx} and ε_2^{yy}. This holds especially for the peaks at ≈ 2.8 eV (Ge substrate) and 3.3 eV (Si), which stem from $v1$ to $c1$ transitions along the R–M line.

Due to the complicated effects of the strain, it is not easy to compare the transitions of SLS's with different substrates. Nevertheless, we think it is important to try to account for some differences in terms of simple linear deformation potential theory. While this might be an oversimplification for some states, it is an approach that works well for the transitions which remain "bulklike," as, for example, the E_2 transitions.[13] Strain effects can be separated into hydrostatic and pure shear components.

A. Hydrostatic strain

If we neglect confinement effects and average the splitting of states due to the uniaxial strain, the simplest ansatz for the hydrostatic energy shift of the transition E_i in a $(Ge)_n/(Si)_m$ SLS under different strain conditions of the Ge and Si layers (i.e., for different $\bar{a}$) is

$$\Delta E_i = 3\left(\frac{n}{n+m} a_i^{\mathrm{Ge}} \epsilon_h^{\mathrm{Ge}} + \frac{m}{n+m} a_i^{\mathrm{Si}} \epsilon_h^{\mathrm{Si}}\right). \qquad (5)$$

Here, a_i are the corresponding deformation potentials for the E_i transition. This approach implies an equal contribution of each Ge and Si atom to E_i (this is justified below). This energy difference should only be valid for SLS's of the *same period* on *different* substrates, as the predictions would become distorted due to different confinement effects for different periods. This can be demonstrated for the E_0 transitions of the $(Ge)_n/(Si)_n$, $n = 2, 4$ SLS, which differ by ≈ 0.06 eV.

Using the DP's from Ref. 20 and Eq. (5), we obtain $\Delta E_0 = 0.58$ eV, when we compare the $[(Ge)_4/(Si)_4]/Si$ to the $[(Ge)_4/(Si)_4]/Ge$ case. This compares rather favorably with the value we obtain from the LMTO calculation: $\Delta E_0 = 0.50$ eV, after averaging over the split Γ_{15}^v bands. Let us briefly consider effects of confinement on the electronic states involved in the E_0 transition: the Γ_{15}^v states are moderately confined in the Ge layers. In the Si substrate case, the VBT (v_1) is 62% confined in the Ge region, while in the Ge substrate case, we obtain 54%. The s states that map onto the Γ_2' conduction band of the bulk materials also show such weak confinement effects (61% for Si, 56% for Ge substrate, respectively). Such rather small effects are negligible for most purposes. For a detailed treatment and discussion of confinement effects, see Ref. 15. Our results are basically the same.

The E_1 transitions are complicated by the variety of peaks explained earlier. The complexity involved does not allow a simple treatment in terms of DP's. This holds only partly for the E_2-like transitions. The shift of these transitons due to the hydrostatic compression, however,

is relatively small, as the relevant DP's are only about one third of those of the E_0 gap.[40] The shift of the E_2 transitions from Ge to Si substrate obtained from our LMTO calculations ($\Delta E_2 = 0.10$ eV) compares reasonably with that predicted by Eq. (5) (0.18 eV).

The sum rule for $\varepsilon_2(\omega)$ should yield N_v, the density of valence electrons,[41] which contribute to all transitions below ω_M:

$$N_v = \frac{1}{2\pi^2}\int_0^{\omega_M} \omega' \varepsilon_2 \, d\omega'. \tag{6}$$

In order for N_v to represent the total density of valence electrons, the integration limit ω_M has to be chosen such that the oscillator strength of the valence electrons is exhausted, while that of the core electrons does not yet play a role. For $\omega_M = 13.6$ eV and using the ε_2's from our LMTO calculations, we find values of N_v that correspond to ≈ 3 electrons/atom (instead of 4), which is also what we obtain for the bulk materials. Of considerable importance, however, is the *extrinsic* nature of N_v and thus the *ratio* of the N_v's obtained for the SLS's on Si and Ge substrate, which should equal the reverse ratio of the corresponding unit-cell volumes, i.e., 1.052. This is exactly the LMTO result, if we average over all three polarizations. The individual ratios for $\varepsilon_2^{xx,yy}$ and ε_2^{zz} yield 1.03 and 1.10, respectively. This difference is probably due to the finite cutoff for ω_M in combination with the enhanced magnitude of ε_2^{zz} in the 2.5–3-eV region.

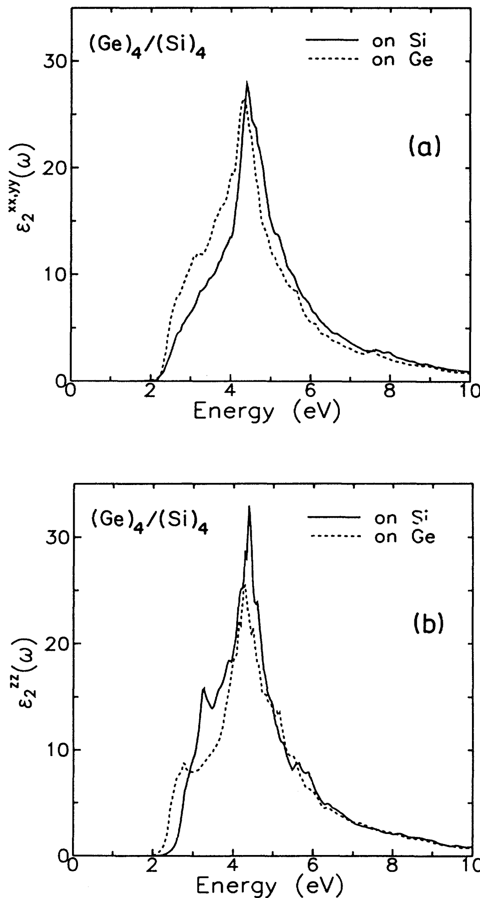

FIG. 7. Comparison of $\varepsilon_2(\omega)$ for $(\mathrm{Ge})_4/(\mathrm{Si})_4$ on Si and on Ge [001] substrate with (a) averaged polarization perpendicular to the growth direction and (b) polarization along [001].

B. Uniaxial strain

The effects of strain on the VBT of diamond and zinc-blende materials have been studied in detail by Pollak and Cardona.[39] For the shift of Γ_{15}^v bands at $\mathbf{k} = \mathbf{0}$ with respect to the weighted average they obtained:

$$E_{v_1} = -\frac{\Delta_0}{6} + \frac{\delta E_{001}}{4} + \tfrac{1}{2}\left(\Delta_0^2 + \Delta_0 \delta E_{001} + \tfrac{9}{4}\delta E_{001}^2\right)^{1/2},$$

$$E_{v_3} = -\frac{\Delta_0}{6} + \frac{\delta E_{001}}{4} - \tfrac{1}{2}\left(\Delta_0^2 + \Delta_0 \delta E_{001} + \tfrac{9}{4}\delta E_{001}^2\right)^{1/2}, \tag{7}$$

$$E_{v_2} = \frac{\Delta_0}{3} - \frac{\delta E_{001}}{2}.$$

Δ_0 is the spin-orbit splitting of the threefold degenerate Γ_{15}^v band into the $|\frac{3}{2}, \pm\frac{3}{2}\rangle$ ($v2$) and the $|\frac{3}{2}, \pm\frac{1}{2}\rangle$ ($v1$) quadruplet and the $|\frac{1}{2}, \pm\frac{1}{2}\rangle$ ($v3$) doublet due to spin-orbit coupling in the absence of strain and δE_{001} the strain splitting. Under the condition of no confinement in either of the Ge or Si layers at the VBT, a simple Vegard-law-type combination of the spin-orbit splittings[12] in Ge ($\Delta_0^{\mathrm{Ge}} \approx 0.30$ eV) and Si ($\Delta_0^{\mathrm{Si}} \approx 0.04$ eV) has been suggested for the SLS's:[4]

$$\Delta_0 = \frac{n}{n+m}\Delta_0^{\mathrm{Ge}} + \frac{m}{n+m}\Delta_0^{\mathrm{Si}}. \tag{8}$$

The additional splitting due to the strain can be treated in the same way.[4] Thus, for a uniaxial strain along the [001] direction, the energy term δE_{001} can be expressed by

$$\delta E_{001} = \frac{n}{n+m} 6 b_{\mathrm{Ge}} \epsilon_u^{\mathrm{Ge}} + \frac{m}{n+m} 6 b_{\mathrm{Si}} \epsilon_u^{\mathrm{Si}}. \tag{9}$$

Here, b_{Ge} and b_{Si} are the uniaxial DP's for Ge and Si, respectively. The theoretical values are given in Ref. 20, together with a discussion of additional relativistic effects. ϵ_u^{Ge} and ϵ_u^{Si} are the uniaxial strain component from Eq. (4) in the Ge and Si layers, respectively.

We have calculated the valence-top splitting for $n = m$ using Eqs. (7)–(9); in this case, all E_{v_i}'s predicted for $n = 1, 2, 3, \ldots,$ are equal. They are shown together with the values obtained from our LMTO calculations for three different substrates as a function of lateral strain in the Si layers ($\epsilon_{\parallel}^{\mathrm{Si}}$) in Fig. 8. The lines calculated with Eqs. (7)–(9) indicate a cross over of the v_2 and the v_1 states for $\epsilon_{\parallel}^{\mathrm{Si}} \approx 2.3\%$. All LMTO values (points) agree well with the analytical results even up to at least $n = 6$.

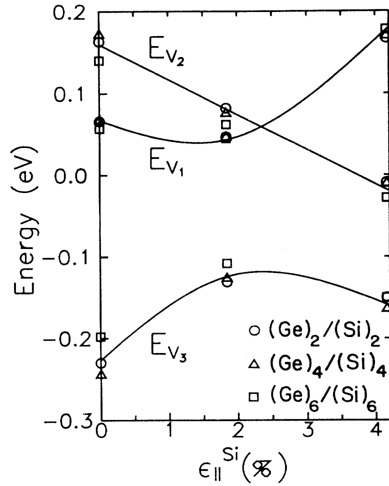

FIG. 8. Splitting of the Γ_{15} top of the valence bands for $(Ge)_n/(Si)_n$ SLS's as a function of lateral strain in the Si layers ($\epsilon_{\|}^{Si}$). The solid lines represent the result of Eqs. (7)–(9), and the symbols the results of the LMTO calculations.

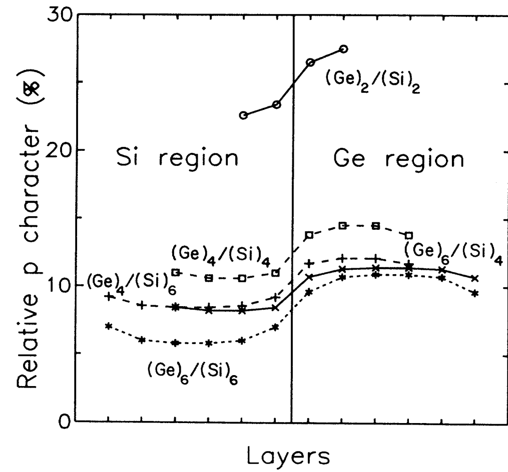

FIG. 9. Relative p contributions of the VBT (averaged over v_1, v_2, and v_3) for various Ge/Si SLS's. The ticks separate individual layers. The interface between the Si and Ge region is indicated by the vertical line.

This can be explained by analyzing the prerequisite for Eqs. (8) and (9), namely the equal spread of the wave functions in the Ge and Si layers, as demonstrated in Fig. 9, where the relative contribution of the p states (the rest is negligible) to the valence-band top, averaged over the three $v1$, $v2$, and $v3$ bands, is displayed. The portion confined to the Ge layers increases from 54% to only 62%, when going from $n = 2$ to 6. The splitting of the VBT should be of importance for the interpretation of recent Kronig-Penney type models[1,7] performed for 10-ML SLS's, which will be described in more detail in the next section. The values calculated with this model for these SLS's are shown in Table IV. They agree, in general, rather well with our LMTO calculations and the DP ansatz, although the Kronig-Penney values given by Pearsall *et al.*[5] are a little larger than the other values.

VI. DIRECT-GAP SUPERLATTICES

Recent electroreflectance[5] (ER) and photoluminescence[7] (PL) experiments Ge/Si SLS's with $n + m = 10$ have stimulated interest in the question of whether quasidirect transitions are possible in this material. The 10-ML system is especially suited for obtaining a direct transition as it is expected that the minimum of the conduction band, which occurs at $\approx 0.83X$ in Si, is folded back to $\mathbf{k} = \mathbf{0}$ for a total periodicity of ten.

A. Effects of strain and composition

Besides the proper periodicity, another requirement has to be met in order to obtain a quasidirect transition: the proper strain distribution and thus $a_{\|}$. This is because the uniaxial strain along the [001] direction splits the formerly sixfold degenerate minima along the cubic Δ direction into two equivalent [001] and four [010], [100] minima by the amount[39]

$$\delta E_X = 3\Xi_u^{\Delta}\epsilon_u . \tag{10}$$

Here, Ξ_u is the relevant DP, which is positive for both Si and Ge.[20] Thus, enough tensile strain in the Si layers is needed to lower the minima of the twofold states (which are folded back to Γ) below those of the four other states. This effect is demonstrated in Fig. 10, where the band structures of $(Ge)_6/(Si)_4$ SLS's on three different substrates are presented. In all these cases, the folded back minima map exactly to Γ, but only in the case of the Ge substrate and in the free-standing case this mini-

TABLE IV. Splitting of the top of the valence band ($E_{v_2} - E_{v_1}$) in eV.

	$\epsilon_{\|}^{Si}$ (%)	LMTO	DP theory[a]	Kronig-Penney
$(Ge)_6/(Si)_4$	4.2	0.13	0.15	0.19,[b] 0.13[c]
$(Ge)_4/(Si)_6$	4.2	0.22	0.25	0.21[c]
$(Ge)_4/(Si)_6$	1.4	−0.04	−0.05	≈ 0[c]

[a] From Eqs. (7)–(9).
[b] From Ref. 5.
[c] From Ref. 7.

mum is lower than the ones occurring along the Δ (Γ–X) direction. Due to confinement effects, the splitting δE_X of these states is somewhat larger than what would be expected from a simple DP argument, such as applying Vegard's law to Eq. (10). In addition, δE_X does not vary much with the compositon of the 10-ML SLS's. This is demonstrated in Fig. 11, where the direct ($E_{\Gamma\text{-}\Gamma}$) and the "competing" indirect transitions are plotted as a function of composition and strain. The symbols in the middle of this plot (i.e., with $1.4\% < \epsilon_{\parallel}^{\mathrm{Si}} < 2.3\%$) represent LMTO results for the free standing case (see Table II); the lines connecting the points are just meant as a guide to the eyes. The energy of the quasidirect $E_{\Gamma\text{-}\Gamma}$ transition on Ge substrates decreases with increasing Si content (m) almost linearly [$0.05(m-n)$ eV], but remains constant for Si substrates. This is consistent with a $\approx$ 85% confinement of the ZF conduction-band minimum (CBM) in the Si layers. These states have almost 50% s character, and the remaining half is equally divided into p and d contributions.

In all cases, the lowest conduction bands along the Γ–Z direction disperse upwards, in contrast to the $(Ge)_4/(Si)_4$ system (Fig. 6, compare also Fig. 3). The most dramatic variation of indirect gaps with composition is found for the $E_{\Gamma\text{-}N}$ gap. It shows a linear behavior with increasing Si content both for the Si [$\approx 0.14(m-n)$ eV] and the Ge substrate [$\approx 0.06(m-n)$ eV].

For completeness, we show in Fig. 12 the band structures of the free-standing $(Ge)_5/(Si)_5$ and the $(Ge)_4/(Si)_6$ SLS, which gives in conjunction with

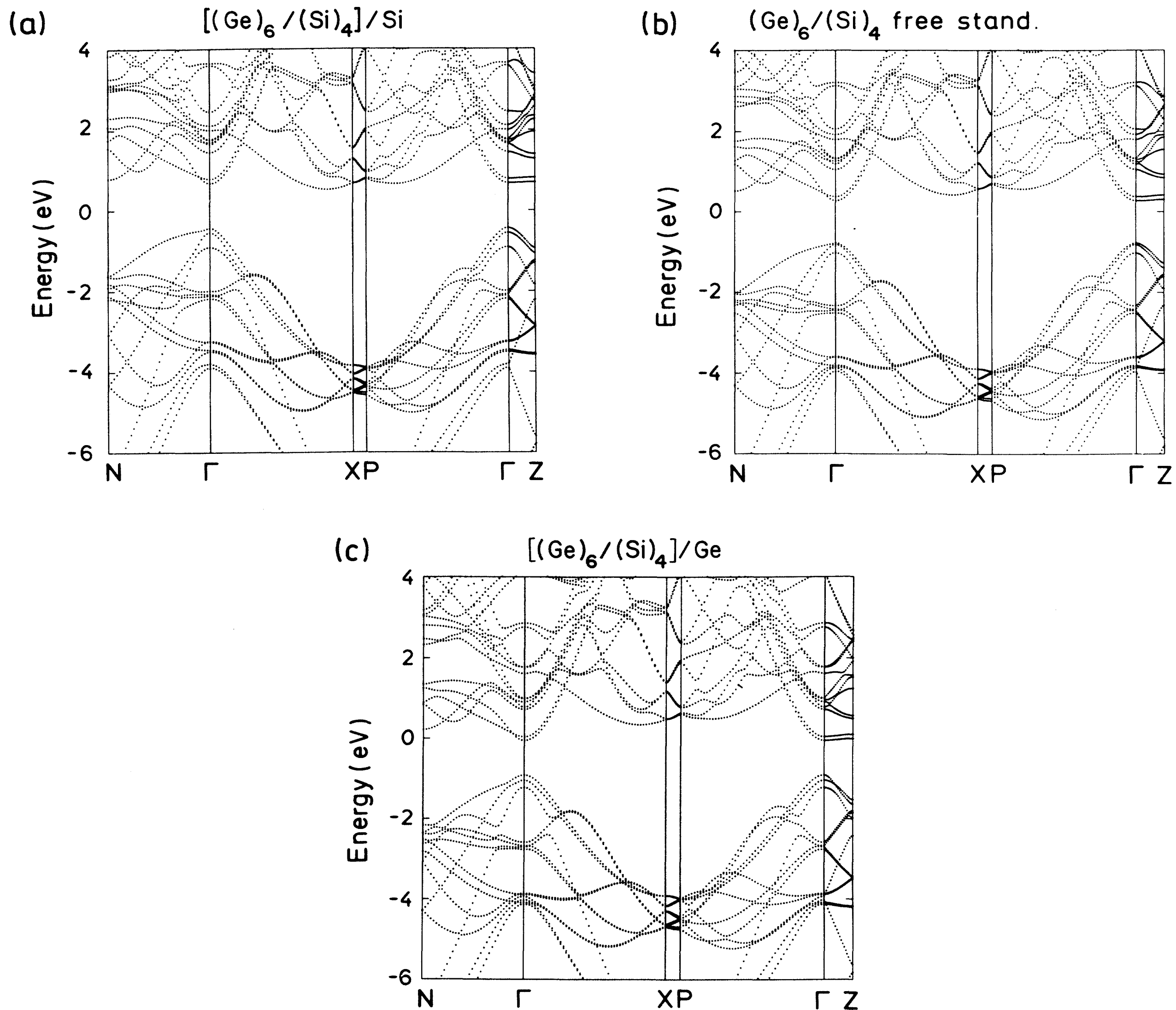

FIG. 10. Electronic band structure of the $(Ge)_6/(Si)_4$ SLS on (a) Si [001] substrate, (b) the free-standing case, and (c) Ge substrate.

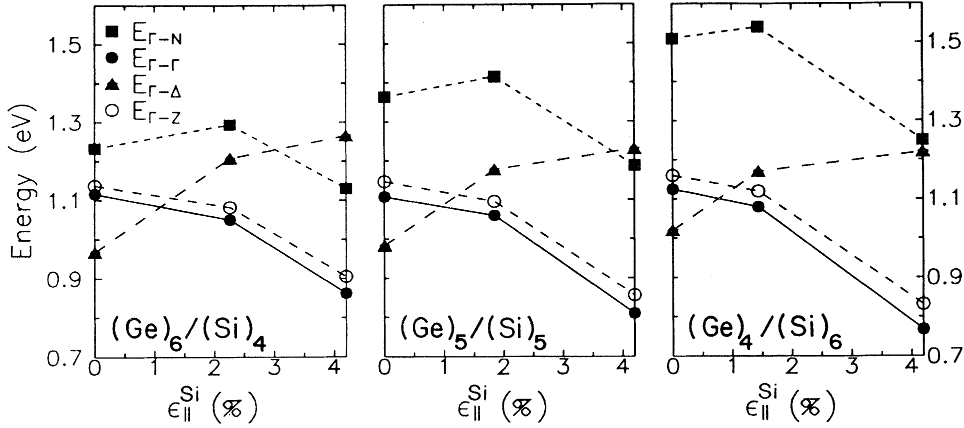

FIG. 11. Transition energies of various 10-ML SLS's as a function of lateral strain in the Si layers. • denotes the *direct* transition energies, in contrast to the competing *indirect* transitions which are also displayed.

Fig. 10(b) a good impression of how a change of n/m affects the eigenvalues. Except for the Γ–N direction, where all bands vary noticeably, the changes are marginal. This reflects the similarity of the bulk band structures in Si and Ge along all lines of symmetry, except for the Γ–N line.

B. Matrix elements and optical response

1. Symmetry, order, and transitions

So far, the conditions for obtaining direct transitions have been derived, regardless whether the lowest direct transitions are optically allowed or not. This issue can only be addressed after a group theoretical analysis of the symmetry properties of the zone-folded bands has been presented.

The 10-ML SLS's with n,m even are rather similar to the $(Ge)_4/(Si)_4$ SLS, for which a detailed group theoretical discussion is given in Ref. 4 (point group D_{2h}). In contrast to the Bouckaert-Smolukowski-Wigner (BSW) notation[42] for the irreducible representations of the point groups used in that paper, we shall use the standard Koster notation[43] for the symmetry analysis in this section. In order to facilitate a comparison of the two notations, the BSW symbols are given in brackets after Koster's in Fig. 13.

While the $(Ge)_4/(Si)_4$ and the 10-ML SLS's with n, m =even share the same point group (D_{2h}), the symmetries of the states folded back to the Γ point vary due to the difference in periodicity and BZ (primitive and body centered, respectively). In the primitive BZ of the $(Ge)_4/(Si)_4$ SLS, the points $(2\pi/a)(0,0,\frac{1}{2})$ and $(2\pi/a)(0,0,1)$ of the diamond BZ are folded back to the Γ point of the superlattice BZ, while in the orthorhombic 10-ML SLS's, these are the points $(2\pi/a)(0,0,\frac{2}{5})$ and $(2\pi/a)(0,0,\frac{4}{5})$. In the cubic BZ, the lowest conduction bands along the [100] direction (Δ) have Δ_1 symmetry. When the compatibility relations to the D_{2h} (D_{2d} for n, m =odd) point group are calculated, they become states with Γ_1^+, Γ_3^- (Γ_1, Γ_3) symmetry. Thus, the two Δ_1 points given above for the cubic BZ will be folded back into four states of the superlattice BZ. In addition, the next conduction states of the cubic $(2\pi/a)(0,0,\frac{4}{5})$ point (Δ_2' states) lie only slightly higher (≈ 0.3 eV) than the higher upper folded Δ_1 states. This is demonstrated in Fig. 13, where the energy bands near the Γ point with their symmetry labels are shown for three free-standing 10-ML Ge/Si SLS's ($4 \leq n \leq 6$). The compatibility relations for the states in this figure are given in Table V. For the convenience of the reader, the dipole-allowed optical transitions to the lowest conduction states are also indicated in Fig. 13 (see Table VI). In this context, there are three especially intriguing points.

(1) Neglecting the slightly different strain states of these SLS's (each of them is free standing, but with different $a_{\parallel}$ and n, m) and confinement effects, one might naively expect the E_0 transition of these SLS's to obey a simple Vegard-type law based on the E_0 transitions of the constituting bulk materials Si and Ge, which vary considerably (4.2 eV and 0.89 eV, respectively). Relativistic effects, however, to which s-like conduction states are especially sensitive,[23] shift these ≈ 0.15 eV below the "Vegard's-law" value.

(2) As described above, we consider four low-lying states originating from the zone-folded, cubic Δ_1 and two from the folded Δ_2' state (the other two Δ_2' 's are beyond the range of Fig. 13). The compositional dependence of the cubic Γ_2' s-like state (Γ_3^- in the D_{2h} group, see Table V) is rather large, as discussed above. In the $(Ge)_4/(Si)_6$ SLS, it occurs at 2.6 eV as $c7$ *after* the six zone-folded states, whereas in the $(Ge)_6/(Si)_4$ SLS, it ranks as $c4$ at 2.0 eV, separating the zone-folded states. The energies of the higher lying bands originating from cubic Γ_{15} states should not be very well represented by our calculation, a shortcoming of the external potentials used in our calculation, well known from our bulk calculations.[12]

(3) Most interesting, however, is the reversal of the two

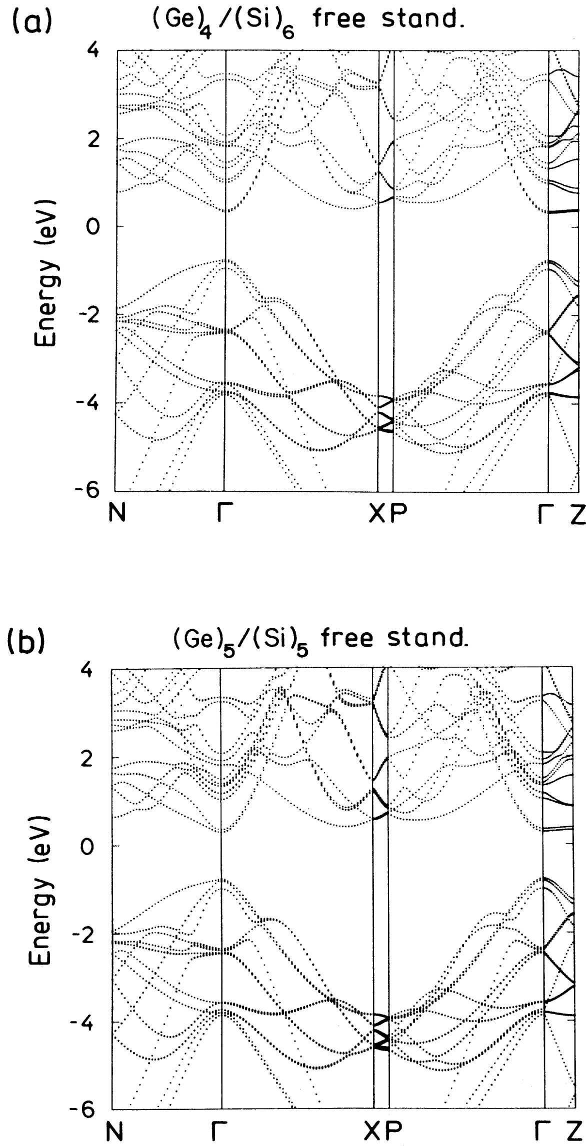

FIG. 12. Band structure of the free-standing (a) $(Ge)_4/(Si)_6$ and (b) $(Ge)_5/(Si)_5$ superlattice along lines of high symmetry. See also Fig. 10(b).

lowest, almost degenerate conduction states, when going from the $n = 4$ to the $n = 6$ SLS. This means that for the $(Ge)_4/(Si)_6$ SLS, the CBM has Γ_3^- symmetry and thus the transition from the VBT to that state is dipole allowed, whereas it is forbidden for the $(Ge)_6/(Si)_4$ case, just as in the $(Ge)_4/(Si)_4$ SLS[4] (see Fig. 13). The magnitude of the allowed matrix element, however, is $\approx 3-4$ orders smaller than that of the *bona fide* E_0 transition at 2.6 eV. Its small value prevents us from giving detailed numbers other than just the order of magnitude, since our calculation diverges for $\mathbf{k} \rightarrow \mathbf{0}$ (an artifact) and the matrix elements should depend on $\mathbf{k}$. The extrapolation method we use, calculating the matrix elements at various points very close to $\mathbf{k} = \mathbf{0}$, has its natural limitations. Nevertheless, we have been able to determine that the matrix element of the direct-gap transiton in the Ge_5Si_5 SLS is only $1 - 2$ orders below that of the E_0 transitions, and thus rather sizable. This is because the D_{2d} point group, in contrast to the D_{2h} group, lacks a center of inversion.[44] The first allowed direct transition of the $(Ge)_6/(Si)_4$ SLS, i.e., the one to the second conduction state, also has a matrix element only approximately equal to two orders of magnitude below that of the E_0 transition.

The reversal of the Γ_3^- and Γ_1^+ states for $m = 4$ compared to $m = 6$ has its origin in the magnitude of the contribution of the s character in the two additional Si layers, which is almost vanishing. Since the electronic states are strongly confined in the Si region, the relative confinement per Si layer decreases with increasing m. Curiously, the higher of these two states shows somewhat higher confinement (additional 2–3 %) than the lower state in both SLS's, contrary to what one might expect. This balance is so delicate that even weak coupling with higher states can reverse the predicted sequence. We should, however, keep in mind that these two electronic states are separated by only 0.04 eV, which is close to the limit of accuracy of our calculation.

Finally, it should be mentioned that the order of the lowest ZF conduction states does not change with varying substrate, in contrast to the crossing of the v_2 and v_1 state at the VBT top in conjunction with a change of polarization of the lowest direct transitions, as discussed in Sec. V.

TABLE V. Compatibility table between relevant states at Γ and Δ in the diamond and in the $(Ge)_n/(Si)_m$ superlattice structures [Koster's notation (Ref. 43)].

Cubic	n, m even	n, m odd
Γ_{25}'	$\Gamma_1^+, \Gamma_2^+, \Gamma_4^+$	Γ_5, Γ_3
Γ_2'	Γ_3^-	Γ_1
Γ_{15}	$\Gamma_2^-, \Gamma_3^-, \Gamma_4^-$	Γ_5, Γ_3
Δ_1	Γ_1^+, Γ_3^-	Γ_1, Γ_3
Δ_2'	Γ_3^+, Γ_1^-	Γ_2, Γ_4

TABLE VI. Dipole-allowed transitions of the $(\mathrm{Ge})_n/(\mathrm{Si})_m$ superlattice at $\mathbf{k} = \mathbf{0}$ in Koster's notation (Ref. 43). For a more detailed analysis of these transitions, including spin-orbit interaction, see Ref. 4.

$(\mathrm{Ge})_n/(\mathrm{Si})_m$	Point group	Polarization	Allowed transitions
n,m even	D_{2h}	x,y	$\Gamma_1^+,\Gamma_3^+ \leftrightarrow \Gamma_2^-$; $\Gamma_2^+,\Gamma_4^+ \leftrightarrow \Gamma_1^-,\Gamma_3^-$
		z	$\Gamma_1^+ \leftrightarrow \Gamma_3^-$; $\Gamma_2^+ \leftrightarrow \Gamma_4^-$; $\Gamma_4^+ \leftrightarrow \Gamma_2^-$; $\Gamma_3^+ \leftrightarrow \Gamma_1^-$
n,m odd	D_{2d}	x,y	$\Gamma_1,\Gamma_2,\Gamma_3,\Gamma_4 \leftrightarrow \Gamma_5$
		z	$\Gamma_1 \leftrightarrow \Gamma_3$; $\Gamma_4 \leftrightarrow \Gamma_2$; $\Gamma_5 \leftrightarrow \Gamma_5$

2. Linear optical response

Figure 14(a) shows the dielectric response of what we believe to be the best candidate for optoelectronic applications, the strain-symmetrized $(\mathrm{Ge})_5/(\mathrm{Si})_5$ SLS. The onset of the absorption due to the allowed direct transitions at ≈ 1.1 eV in $\varepsilon_2^{xx,yy}$ is magnified by a factor of 10^3, thus allowing us to compare the calculated oscillator strengths. The 5×5 structure on the Ge substrate has slightly smaller matrix elements for p_z polarization than the free-standing one, but in addition has to cope with the problem of critical thickness.[2]

The calculated linear optical response of the type of SLS that has been grown by Pearsall *et al.*[5] is displayed in Fig. 14(b). As this SLS is on the Ge substrate, the quasidirect transitions from the VBT are p_z polarized, which is easy to discern in the blow up. The spectra of both of these SLS's show a rich structure. For a detailed analysis of these structures in a symmetrically strained $(\mathrm{Ge})_4/(\mathrm{Si})_6$ SLS in terms of interband transitions and a comparison to experimental data, see Ref. 13.

3. Comparison with experiment

Table VII shows a comparison of recent experimental results on 10-ML SLS's grown on various substrates and our LMTO calculations of the direct transitions. Let us first discuss the electroreflectance and photoreflectance data of Asami and co-workers[45] for Ge/Si SLS's on the Si [001] substrate. The periodic structure has been repeated only six times, i.e., the samples grown can be described as $[(\mathrm{Ge})_n/(\mathrm{Si})_m]_6$; thus we have to be careful when comparing our calculations, which are based on infinitely repeating structures. As demonstrated in

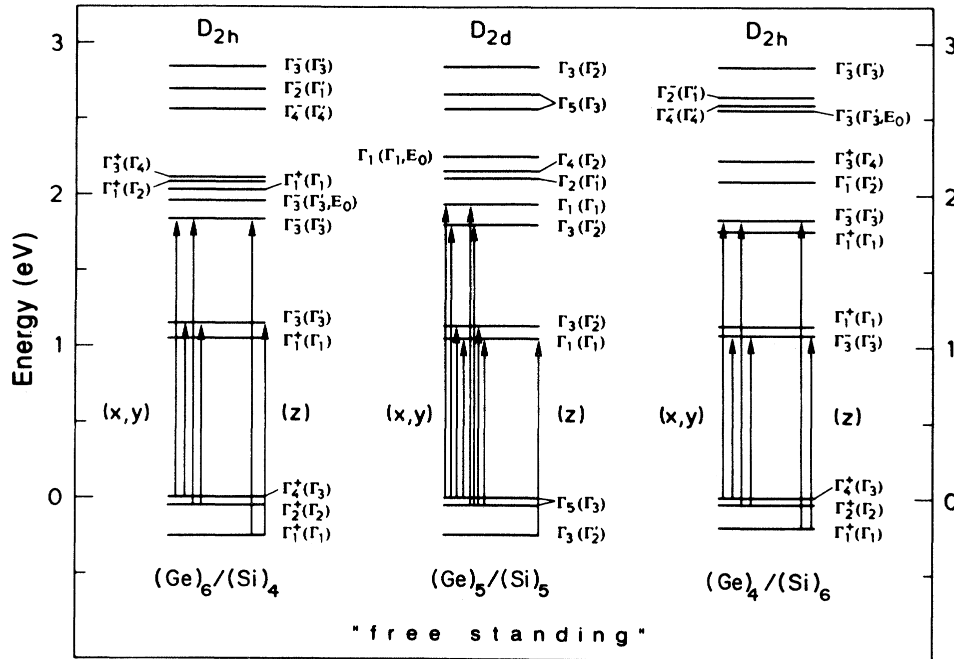

FIG. 13. Symmetry and order of the energy levels at the Γ point of the three 10-ML SLS's covered in the text. Note that we use Koster's notation (Ref. 43) for symmetry labeling, with the BSW notation (Ref. 42) added in parentheses. The dipole-allowed transitions are given for clarity only for the four lowest states, the rest can be supplemented using Table VI.

the preceding sections, these SLS's have an indirect gap at $\approx 0.95 - 1.05$ eV. The experimental data show two transitions below the direct ones, of which one could in analogy to the $(Ge)_4/(Si)_4$ case be assigned to the lowest indirect transition. The other peak has been observed for the first time [analogous to the $(Ge)_4/(Si)_4$ sample, in which the authors of Ref. 45 found a similar peak that has not been reported in Ref. 1] and on the basis of our theoretical calculations no explanation can be given. The measured spectra of both the $(Ge)_4/(Si)_6$ and the $(Ge)_6/(Si)_4$ sample are very much alike, a fact that suggests that there must be a considerable amount of interface diffusion. While our calulation reproduces the lowest direct transitions quite well (disregarding the reversal of the lowest allowed and not allowed transitions, that accounts for most of the change of the transitions energies, which would otherwise be almost identical) the higher-lying folded transitions have not been detected experimentally. In addition, the shift of the rather strong E_0 peak with composition could not be verified either. Such a shift, however, has to occur independently of the type of calculation, and the fact that such a strong feature could not be detected experimentally leaves serious doubts as to whether a direct comparison of the experimental results with the calculations are valid at all.

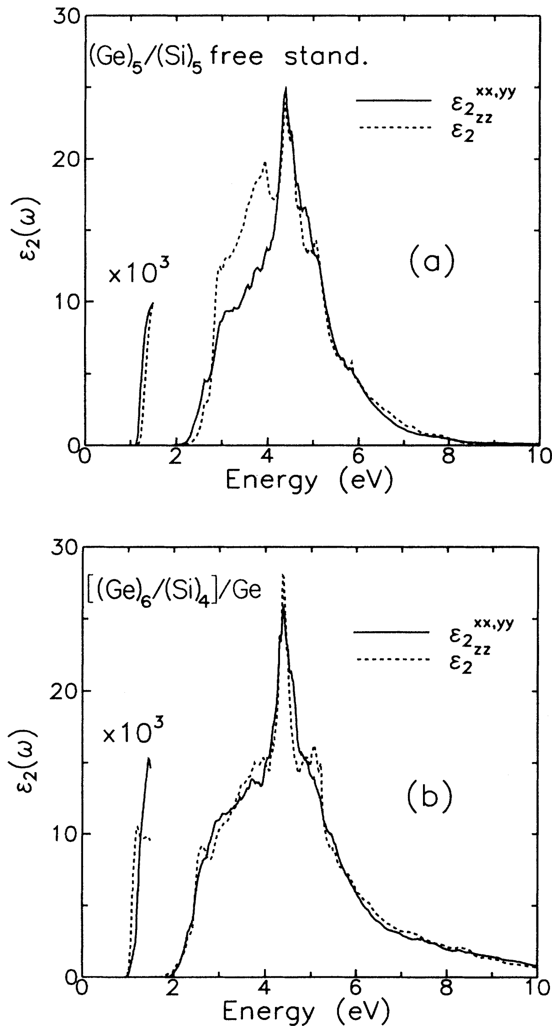

FIG. 14. Linear optical response of (a) the free-standing $(Ge)_5/(Si)_5$ and (b) the $[(Ge)_6/(Si)_4]/Ge$ SLS. Note that the energy region up to 1.5 eV has been magnified by a factor of 10^3 in order to clearly observe the absorption due to the (quasi)direct transitions.

Turning to the electroreflectance experiment by Pearsall *et al.* on the $[(Ge)_6/(Si)_4]/Ge$ sample,[5] it should be mentioned that in their geometry they could not excite the lowest direct transition, which occur in p_z polarization. The lowest transitions for both p_z (at 0.86 eV from v_1) and $p_{x,y}$ polarization (at 0.99 eV from v_2) are *forbidden*, as the CBM has Γ_1 symmetry. This finding is in contradiction with the statement by Pearsall,[5] based on empirical pseudopotential calculations by Gell.[19] The first calculated, *allowed* transition in $p_{x,y}$ polarization occurs at 1.09 eV and is in good agreement with the experimental result of 0.96 eV. It can also be argued, that a small perturbation, such as misalignment or roughness at the interface, may suffice to transform a *forbidden* transition into an *allowed* one. In that case, we would have to compare the experimental 0.96 eV with 0.99 eV. Anyway, we always have to keep in mind that our calculations are concerned with *idealized* SLS's, and *ab initio* studies of interdiffused SLS's models require an enormous computational effort, and can be considered to be still in their infancy.[44,46]

This also holds for the last experiment we want to discuss, the photoluminescence measurement by Zachai *et al.*[7] on a strain-symmetrized $(Ge)_4/(Si)_6$ sample, one of the most debated experimental results. In that case, our calculations indicate that the lowest transition from the CBM to the VBT is allowed (see Fig. 13). We have pointed out earlier[8] that the measured value of 0.84 eV is well below the calculated energy of 1.1 eV, and suggested that the observed peak could be related to defects, in particular misfit dislocations, which are contained at high densities in the sample. Recently, there has been experimental support for this interpretation by Northrop *et al.*[47] A Canadian group,[48] however, found in their PL experiments that neither zone-folding effect nor misfit dislocations are needed in order to produce PL peaks similar in shape and energy to the ones found in Ref. 7. The exact origin of these transitions remains an open question.

VII. CONCLUSIONS

We have applied *ab initio* calculations with an *ad hoc* correction to the LDA "band-gap problem" in order to obtain the band structures and linear optical response of a variety of Ge/Si superlattices. The results obtained with this method are almost identical with the state-of-the-art quasiparticle calculations,[15] which have only been carried out for one SLS. Also, to our knowledge, no such

TABLE VII. Comparison of calculated and measured direct transitions in 10-ML SLS's. All energies are in eV. The energies given here are from a *fully relativistic* calculation, including spin-orbit interaction. The notation of the eigenstates, however, refers to the single group, i.e., with spin-orbit coupling neglected.

	$\epsilon_{\parallel}^{\mathrm{Si}}$ (%)	Experimental	LMTO	Transition
$(Ge)_4/(Si)_6$	0.0	1.22[a]	1.13	$\Gamma_4^+ \rightarrow \Gamma_3^-$ $(p_{x,y})$
			1.85	$\Gamma_4^+ \rightarrow \Gamma_3^-$ $(p_{x,y})$
		2.10[a]	2.14	$\Gamma_4^+ \rightarrow \Gamma_1^-$ $(p_{x,y})$
			2.68	$\Gamma_4^+ \rightarrow \Gamma_3^-$ $(E_0, p_{x,y})$
$(Ge)_6/(Si)_4$	0.0	1.25[a]	1.22	$\Gamma_4^+ \rightarrow \Gamma_3^-$ $(p_{x,y})$
			1.89	$\Gamma_4^+ \rightarrow \Gamma_3^-$ $(p_{x,y})$
		2.10[a]	2.10	$\Gamma_4^+ \rightarrow \Gamma_3^-$ $(E_0, p_{x,y})$
			2.19	$\Gamma_4^+ \rightarrow \Gamma_1^-$ $(p_{x,y})$
$(Ge)_6/(Si)_4$	4.2		0.96[d]	$\Gamma_1^+ \rightarrow \Gamma_3^-$ (p_z)
		0.96[b]	1.09[d]	$\Gamma_2^+ \rightarrow \Gamma_3^-$ $(p_{x,y})$
$(Ge)_4/(Si)_6$	1.4	0.84[c]	1.08[e]	$\Gamma_{2,4}^+ \rightarrow \Gamma_3^-$ $(p_{x,y})$
		0.84[c]	1.12	$\Gamma_1^+ \rightarrow \Gamma_3^-$ $(p_{x,y})$

[a]Electroreflectance and photoreflectance, from Ref. 45.
[b]Electroreflectance, from Ref. 5.
[c]Photoluminescence, from Ref. 7, see text.
[d]Inclusion of spin-orbit interaction causes the v_1 state to be at the VBT and thus the lowest energy also occurs in p_z polarization.
[e]Inclusion of spin-orbit interaction turns the Γ_4^+ (Γ_2^+) into the v_2 (v_1) state $(E_{v_1} > E_{v_2}$, see Fig. 8). The lower transition from v_1 then has a p_z component.

calculation which includes spin-orbit interaction or yields the dielectric response has been reported.

Of special interest has been the anisotropy of the dielectric response of the orthorhombic SLS's. While the $(x, y) - z$ anisotropy should be experimentally accessible once sufficiently thick samples are available so that spectroscopic methods such as ellipsometry can be applied, the detection of the x, y anisotropy will remain elusive unless the perfection with which these SLS's are grown reaches the point, where hundreds of periods can be grown within a precision of only one ML per period. The introduction of just one additional monoatomic step is expected to destroy the (x, y) anisotropy, which has so far been undetectable.[13] In addition, interface diffusion may deteriorate the optical anisotropy of otherwise perfect SLS's. The shift of optical peaks due to difference in strain, as has been calculated in Sec. V, should stimulate further experiments. A clear downshift in energy of photoluminescence spectra with increasing lateral strain in Si layers $(\epsilon_{\parallel}^{\mathrm{Si}})$ has already been observed.[7]

Further experimental evidence for the calculated splitting of the VBT due to the internal strain should be possible by means of electroreflectance and photoreflectance experiments. It has been shown that a simple Vegard-type law agrees well with our elaborate fully relativistic calculations, after spin-orbit coupling has been included.

Conditions for obtaining (quasi)direct transitions have been derived. The situation has shown to be rather complex, especially the question of whether the lowest folded back conduction states yield allowed transitions from the VBT or not. We thus included a group theoretical discussion of the symmetry properties of these and various other states. Our statements concerning the matrix elements had to be rather vague and could not be more precise than their magnitude. Here, spin-orbit effects play a minor role. They do cause some more transitions to become allowed, but the magnitude of these additional transitions is extremely weak.[4] Moreover, the *fundamental* transitions which concern us most will be unaffected by this refinement.

Not all experiments we discussed in Sec. VI B showed the entire features which we calculated. This may partly be due to the fact that we are calculating an idealized system that does not include essential effects such as interface mixing. Also, some of the measurements have been done under different conditions, such as temperature. Our calculations do not include temperature shift. The experimental results are also clearly affected by the quality of some samples, which still has to be improved for a direct comparison with calculations. Almost identical experiments performed on samples of different source and thus different method of growth, preparation, or thickness—or even only of a different series of the same source—often do not yield identical results. We realize

how difficult it is both to grow these SLS's and to interpret relevant experiments.

On the other hand, *ab initio* simulations of some deficiencies of the samples, such as interface diffusion, have already been reported.[44] Further theoretical progress can be expected from such calculations, which represent an elegant but computationally demanding approach of modeling "real" systems.

Despite all these shortcomings, the overall agreement of the experiments and our calculations is rather satisfactory, most differences being smaller than 0.1 eV. The $(Ge)_5/(Si)_5$ system has been predicted to be the most suitable candidate for optoelectronic applications of all SLS's studied here. The future will show whether such devices are actually feasible.

ACKNOWLEDGMENTS

We thank I. Gorczyca for her help with the Keating model, G. La Rocca for his advice in group theoretical matters, and O.K. Andersen for fruitful discussions. S. Satpathy's clarifying remarks about the symmetry notation of the eigenstates is acknowledged. This work has also benefited from discussions with the workers of the groups in Ulm (Daimer Benz Research Institute) and Munich (W. Schottky Institute), in particular, E. Kasper, H. Presting, R. Zachai, K. Eberl, M. Dahmen, and G. Abstreiter. We are also indebted to the Höchstleistungrechenzentrum in Jülich, Germany, for providing us with a supercomputer time grant on their CRAY Y-MP8/832 computer.

---

*Also at Institute of Physics, Aarhus University, DK-8000 Aarhus C, Denmark.

†Present address: Los Alamos National Laboratory, Los Alamos, NM 87545.

[1] T.P. Pearsall, J. Bevk, L.C. Feldman, J.M. Bonar, J.P. Mannaerts, and A. Ourmazd, Phys. Rev. Lett. **58**, 729 (1987); T.P. Pearsall, J. Bevk, J.C. Bean, J. Bonar, J.P. Mannaerts, and A. Ourmazd, Phys. Rev. B **39**, 3741 (1989), and references cited therein.

[2] E. Kasper, H. Kibbel, H. Jorke, H. Brugger, E. Friess, and G. Abstreiter, Phys. Rev. B **38**, 3599 (1988).

[3] U. Gnutzmann and K. Clausecker, Appl. Phys. **3**, 9 (1974).

[4] S. Satpathy, R.M. Martin, and C.G. Van de Walle, Phys. Rev. B **38**, 13 237 (1988). Note that in Table II the $\Gamma_3 \leftrightarrow \Gamma_3$ transition (BSW notation) in z polarization should be contained for the D_{2d} point group. The authors agree on that point.

[5] T.P. Pearsall, J.M. Vandenberg, R. Hull, and J.M. Bonar, Phys. Rev. Lett. **63**, 2104 (1989).

[6] R. Zachai, E. Friess, G. Abstreiter, E. Kasper, and H. Kibbel, in *Proceedings of the Nineteenth International Conference on the Physics of Semiconductors*, edited by W. Zawadzki (Warschau, Poland, 1988), p. 487; G. Abstreiter, K. Eberl, E. Friess, W. Wegschneider, and R. Zachai, J. Cryst. Growth **95**, 431 (1989).

[7] R. Zachai, K. Eberl, G. Abstreiter, E. Kasper, and H. Kibbel, Phys. Rev. Lett. **64**, 1055 (1990).

[8] U. Schmid, N.E. Christensen, and M. Cardona, Phys. Rev. Lett. **65**, 2610 (1990).

[9] O.K. Andersen, Phys. Rev. B **12**, 3060 (1975).

[10] D. Glötzel, B. Segal, and O.K. Andersen, Solid State Commun. **36**, 403 (1980).

[11] N.E. Christensen, Phys. Rev. B **30**, 5753 (1984).

[12] U. Schmid, N.E. Christensen, and M. Cardona, Phys. Rev. B **41**, 5919 (1990).

[13] U. Schmid, F. Lukeš, N.E. Christensen, M. Alouani, M. Cardona, E. Kasper, H. Kibbel, and H. Presting, Phys. Rev. Lett. **65**, 1933 (1990).

[14] C.G. Van de Walle and R.M. Martin, Phys. Rev. B **34**, 5621 (1986); J. Vac. Sci. Technol. B **3**, 1256 (1985).

[15] M.S. Hybertsen and M. Schlüter, Phys. Rev. B **36**, 9683 (1987); M.S. Hybertsen, M. Schlüter, R. People, S.A. Jackson, D.V. Lang, T.P. Pearsall, J.C. Bean, J.M. Vandenberg, and J. Bevk, *ibid.* **37**, 10 195 (1988); P. Friedel, M.S. Hybersten, and M. Schlüter, *ibid.* **39**, 7974 (1989); M. Schlüter and M.S. Hybertsen, in *Progress on Electron Properties of Solids*, edited by R. Girlanda *et al.* (Kluwer, Amsterdam, 1989).

[16] S. Froyen, D.M. Wood, and A. Zunger, Phys. Rev. B **36**, 4547 (1987); **37**, 6893 (1988).

[17] S. Ciraci and I.P. Batra, Phys. Rev. Lett. **58**, 2114 (1987); Phys. Rev. B **38**, 1835 (1988).

[18] I. Morrison, M. Jaros, and K.B. Wong, Phys. Rev. B **35**, 9693 (1987).

[19] M. Gell, Phys. Rev. B **38**, 7535 (1988).

[20] U. Schmid, N.E. Christensen, and M. Cardona, Solid State Commun. **75**, 39 (1990).

[21] M.I. Alonso, M. Cardona, and G. Kanellis, Solid State Commun. **69**, 479 (1989); **70**, i (1989).

[22] E. Ghahramani, D.J. Moss, and J.E. Sipe, Phys. Rev. B **41**, 5112 (1990); **42**, 9193(E) (1990), where the $x-y$ anisotropy is given as an off-diagonal element of "ε" referred to the cubic axes.

[23] G.B. Bachelet and N.E. Christensen, Phys. Rev. B **31**, 879 (1985).

[24] I. Gorczyca, N.E. Christensen, and M. Alouani, Phys. Rev. B **39**, 7705 (1990); I. Gorczyca and N.E. Christensen, Solid State Commun. **72**, 785 (1989).

[25] M. Alouani, S. Gopalan, M. Garriga, and N.E. Christensen, Phys. Rev. Lett. **61**, 1643 (1988).

[26] M. Alouani, L. Brey, and N.E. Christensen, Phys. Rev. B **37**, 1167 (1988). As in this paper, we omitted spin-orbit (s.o.) coupling in the calculaton of $\varepsilon_2(\omega)$. The built-in strain splits the bands to an extent, which exceeds any s.o. effects.

[27] O. Jepsen and O.K. Andersen, Solid State Commun. **9**, 1763 (1971).

[28] P. Molinàs i Mata, M.I. Alonso, and M. Cardona, Solid State Commun. **74**, 347 (1990).

[29] K.B. Wong, M. Jaros, I. Morrison, and J.P. Hagon, Phys. Rev. Lett. **60**, 2221 (1988); C.G. Van de Walle, *ibid.* **62**, 974 (1989); S. Froyen, D.M. Wood, and A. Zunger, *ibid.* **62**, 975 (1989); M. Jaros, *ibid.* **62**, 976 (1989).

[30]S. Ciraci, A. Baratoff, and I.P. Batra, Phys. Rev. B **41**, 6069 (1990).
[31]J. Zi, K. Zhang, and X. Xie, Appl. Phys. Lett. **57**, 165 (1990).
[32]A. Qteish and E. Molinari, Phys. Rev. B **42**, 7090 (1990).
[33]R. People, Phys. Rev. B **32**, 1405 (1985).
[34]P.N. Keating, Phys. Rev. **145**, 637 (1966).
[35]R.M. Martin, Phys. Rev. B **1**, 4005 (1970).
[36]L.C. Feldman, J. Bevk, B.A. Davidson, H.J. Gossmann, and J.P. Mannaerts, Phys. Rev. Lett. **59**, 664 (1987); see, however, S. A. Chambers and V. A. Loebs, Phys. Rev. B **42**, 5109 (1990). These authors determine average $a_\perp$ which agree well with the *ab initio* data of Ref. 16, but not with the fully relaxed calculations of Ref. 30.
[37]This is consistent with the results of Froyen, Wood, and Zunger (Ref. 16) but contradicts the calculations of Ciraci, Baratoff, and Batra (Ref. 30). As our model does not take into account charge transfer across the interface, we can exclude this as a possible explanation for the "overshoot" of the Ge-Ge distances at the interface, as has been conjectured by Froyen, Wood, and Zunger (Ref. 16).
[38]A.P. Cracknell, B.L. Davies, S.C. Miller, and W.F. Love, *Kronecker Product Tables* (Plenum, New York, 1979), Vol. 1.
[39]F.H. Pollak and M. Cardona, Phys. Rev. **172**, 816 (1968); L.D. Laude, F.H. Pollak, and M. Cardona, Phys. Rev. B **3**, 2623 (1971); M. Chandrasekhar and F.H. Pollak, *ibid.* **15**, 2127 (1977).
[40]In this case, we refer to the experimental deformation potentials (Ref. 39) $a(E_2^{\mathrm{Si}}) = -2.9$ eV and $a(E_2^{\mathrm{Ge}}) = -4.2$ eV.
[41]M. Cardona, in *Atomic Structure and Properties of Solids*, edited by E. Burstein (Academic, New York, 1972), p. 541.
[42]L.P. Bouckaert, R. Smolukowski, and E. Wigner, Phys. Rev. **50**, 58 (1936).
[43]G.F. Koster, J.O. Dimmock, R.G. Wheeler, and H. Statz, *Properties of the Thirty-two Point Groups* (MIT, Cambridge, MA, 1963); G.F. Koster, in *Solid State Physics*, edited by F. Seitz and D. Turnbull (Academic, New York, 1957), p. 173.
[44]M. Ikeda, K. Terakura, and T. Oguchi, in *Proceedings of the Twentieth International Conference of the Physics of Semiconductors*, edited by E.M. Anastassakis and J.D. Joannopoulos (Thessaloniki, Greece, 1990), p. 889.
[45]K. Asami, K. Miki, K. Sakamoto, T. Sakamoto, and S. Gonda, Jpn. J. Appl. Phys. **29**, L 381 (1990).
[46]M.D. Sturge and M.-H. Meynadier, J. Lumin. **44**, 199 (1989).
[47]G.A. Northrop, S.S. Iyer, and D.J. Wolford, in *Impurities, Defects and Diffusion in Semiconductors: Bulk and Layered Structures*, edited by D. J. Wolford, J. Bernholc, and E. E. Haller, MRS Symposia Proceedings No. 163 (Materials Research Society, Pittsburgh, 1990), p. 343; G.A. Northrop, D.J. Wolford, S.S. Iyer, and V.P. Kesan, in Ref. 44, p. 857.
[48]J.-P. Noël, N.L. Rowell, D.C. Houghton, and D.D. Perovic, Appl. Phys. Lett. **57**, 1037 (1990); D.C. Houghton, J.-P. Noël, and N.L. Rowell, Mater. Sci. Engin. B (to be published). See also J. C. Sturm, H. Manoharan, L. C. Lenchyshyn, M. L. W. Thewalt, N. L. Rowell, J.-P. Noël, and D. C. Houghton, Phys. Rev. Lett. **66**, 1362 (1991).